Pseudopilin residue E5 is essential for recruitment by the type 2 secretion system assembly platform.

Mangayarkarasi Nivaskumar, Javier Santos-Moreno, Christian Malosse, Nathalie Nadeau, Julia Chamot-Rooke, Guy Tran van Nhieu, Olivera Francetic

Pseudopilin residue E5 is essential for recruitment by the type 2 secretion system assembly platform

Mangayarkarasi Nivaskumar[1,2#]*, Javier Santos-Moreno[2-6,*], Christian Malosse[7], Nathalie Nadeau[1], Julia Chamot-Rooke[7], Guy Tran Van Nhieu[3-6] and Olivera Francetic[1,8]

[1]Laboratory of Macromolecular Systems and Signalling, Institut Pasteur, Department of Microbiology, CNRS ERL3526, 25 rue du Dr Roux, 75724 Paris, Cedex 15, France

[2]Université Paris Diderot (Paris 7) Sorbonne Paris Cité

[3]Laboratory of Intercellular Communication and Microbial Infections, CIRB, Collège de France, Paris France

[4]Institut National de la Santé et de la Recherche Médicale (Inserm) U1050, France

[5]Centre National de la Recherche Scientifique (CNRS), UMR7241, France

[6]MEMOLIFE Laboratory of Excellence and Paris Science Lettre, France

[7]Structural Mass spectrometry and Proteomics unit, CNRS UMR3528, Institut Pasteur, Paris, France

[#]Present address: Department of Chemistry, National University of Singapore, 3 Science Drive, Singapore 117543

* Co-first authors

[8]Correspondence: ofrancet@pasteur.fr

Tel: 33 1 40 61 36 81

Fax: +33 1 45 68 89 60

Running title: Pseudopilin interactions with assembly factors

Key words: type 2 secretion system, type 4 pili, pilus assembly, bacterial two-hybrid, assembly platform, protein interactions

Summary

Type II secretion systems (T2SSs) promote secretion of folded proteins playing important roles in nutrient acquisition, adaptation and virulence of Gram-negative bacteria. Protein secretion is associated with the assembly of type 4 pilus (T4P)-like fibres called pseudopili. Initially membrane embedded, pseudopilin and T4 pilin subunits share conserved transmembrane segments containing an invariant Glu residue at the 5th position, E5. Mutations of E5 in major T4 pilins and in PulG, the major pseudopilin of the *Klebsiella* T2SS abolish fibre assembly and function. Among the four minor pseudopilins, only PulH required E5 for secretion of pullulanase, the substrate of the Pul T2SS. Mass-spectrometry analysis of pili resulting from the co-assembly of $PulG^{E5A}$ variant and $PulG^{WT}$ ruled out an E5 role in pilin processing and N-methylation. A bacterial two-hybrid analysis revealed interactions of the full-length pseudopilins PulG and PulH with the PulJ-PulI-PulK priming complex and with the assembly factors PulM and PulF. Remarkably, $PulG^{E5A}$ and $PulH^{E5A}$ variants were defective in interaction with PulM, but not with PulF and co-purification experiments confirmed the E5-dependent interaction between native PulM and PulG. These results reveal the role of E5 in a recruitment step critical for assembly of the functional T2SS, likely relevant to T4P assembly systems.

Introduction

Bacterial interactions with their environment involve the transport of proteins and other macromolecules across their cell envelope. In Gram-negative bacteria, several sophisticated molecular machines facilitate protein secretion across two bilayer membranes (Costa *et al.*, 2015). Among these, the type II secretion system (T2SS) promotes specific transport of folded proteins across the outer membrane once they have reached the periplasmic compartment though the Sec or the Tat systems (Voulhoux *et al.*, 2001; Korotkov *et al.*, 2012; Nivaskumar and Francetic, 2014). T2SSs are structurally and functionally similar to type IV pilus (T4P) assembly systems (Berry and Pelicic, 2014). Unlike type IV pili, which extend beyond the bacterial surface to promote attachment and motility, the T2SS pseudopilus fibres are thought to be restricted to the periplasm. However, plate-cultured bacteria that overexpress T2SS-encoding genes present extended pseudopili (hereafter referred to as T2SS pili) on the cell surface, a feature that has facilitated their biochemical and structural characterisation (Sauvonnet *et al.*, 2000; Durand *et al.*, 2003; Kohler *et al.*, 2004). T2SS pili are helical homo-polymers composed of one major pseudopilin subunit called PulG *in K. oxytoca* (Sauvonnet *et al.*, 2000; Kohler *et al.*, 2004). Mechanistic insights gained from their structure function analysis have revealed that interactions between neighbouring pilus subunits P and P^{+1} tightly correlate with fibre assembly and function in protein secretion (Campos *et al.,* 2010). The fact that these essential contacts take place in the membrane implies a one-start helix rotational assembly mode for these and other type 4 pilus-like fibres (Nivaskumar *et al.,* 2014).

Pseudopilus biogenesis is a multistep process that begins with co-translational insertion of pseudopilins in the inner membrane (IM) *via* the SRP and the Sec machinery (Arts *et al.*, 2007; Francetic *et al.*, 2007). Pseudopilins are made as precursors anchored in the IM through a positively charged N-terminal peptide that is removed prior to assembly by an inner membrane protease called the prepilin peptidase (Nunn and Lory, 1991). Following

cleavage of this peptide after a conserved Gly residue at the base of the transmembrane segment, the N-terminal domain of the prepilin peptidase transfers a methyl group to the new N-terminal residue of the mature pilin (Strom *et al.*, 1993; Aly *et al.*, 2013).

In addition to the highly abundant major pseudopilins that build the helical homo-polymeric fibre, T2SSs contain four minor pseudopilins, essential for function. Purified globular domains of three of these minor subunits, GspI, GspJ and GspK from enterotoxigenic *Escherichia coli* form a quasi-helical complex, which is predicted to cap the pseudopilus tip (Korotkov and Hol, 2008). Functional, biochemical and molecular dynamics analysis of their full-length equivalents in the Pul T2SS showed that PulI, PulJ and PulK self-assemble in the IM in the absence of other T2SS factors (Cisneros *et al.*, 2012a). The PulJ-PulI-PulK complex promotes initiation of pseudopilus assembly and presumably provides a template for subsequent incorporation of PulH and PulG subunits. Mutants lacking PulI, PulJ or PulK, but not PulH, assemble fewer PulG pili and are completely defective for secretion of the specific Pul T2SS substrate, pullulanase (PulA) (Cisneros *et al*., 2012a). Biochemical studies of the *Pseudomonas aeruginosa* Xcp T2SS show that the periplasmic domain of the PulH homologue XcpU forms a complex with other minor pseudopilins *in vitro* by binding to the PulJ homologue XcpW (Yanez *et al.*, 2008; Korotkov and Hol, 2008; Douzi *et al.*, 2009). In addition, the major pseudopilin XpsG of *Xanthomonas campestris* T2SS and the minor subunit XpsH, a PulH homologue, interact directly *in vivo* (Hu *et al.,* 2002). Based on these studies, PulH homologues are thought to provide a link between the priming complex and the major pseudopilins (Yanez *et al*., 2008; Korotkov and Hol, 2008; Douzi *et al*., 2009; Cisneros *et al*., 2012a).

Assembly of PulG fibres requires a functional complex called the assembly platform (AP) composed of the IM proteins PulC, PulF, PulL and PulM (Py *et al.*, 2001; Possot *et al.*, 2000). The cytoplasmic domain of PulL binds the hexameric ATPase PulE that provides energy for pseudopilus assembly (Abendroth *et al.*, 2005; Camberg *et al.*, 2007). Biochemical and structural analyses of AP components in T2SSs have provided molecular insights into their soluble domains and hints about their interactions and organization

(Korotkov *et al.*, 2011; Abendroth *et al.*, 2004b; Abendroth *et al.*, 2004a; Sandkvist *et al.*, 1995; Johnson *et al.*, 2007; Abendroth *et al*., 2005). This information has led to the current T2SS model, where the IM platform promotes pseudopilus assembly within a cage-like compartment delimited by the secretin channel formed by a GspD dodecamer in the outer membrane and the GspD-interacting partner GspC in the IM (Gsp being a generic term to designate T2SS components) (McLaughlin *et al.*, 2012).

The hydrophobic segments of major (pseudo)pilins in bacterial T4P and T2SSs are highly conserved and rich in branched chain amino acid residues. In addition to the conserved Gly residue preceding the prepilin peptidase cleavage site, mature subunits contain an invariant Glu residue at position 5 (E5), which is located near the cytoplasmic side of the transmembrane segment and is essential for function (Strom and Lory, 1991; Aas *et al.*, 2007; Pugsley, 1993). In the T4P systems, residue E5 has been implicated in prepilin processing (Pasloske and Paranchych, 1988) or N-methylation (Strom and Lory, 1991; Aas *et al*., 2007). Based on structural studies of T4P, it has also been proposed that E5 is involved in docking of pilins to the growing fibre during assembly, by forming electrostatic contacts with the N-terminal amine of the last pilin subunit incorporated in the pilus (Parge *et al.*, 1995; Craig *et al.*, 2006).

In contrast, the E5V substitution in PulG from *K. oxytoca* T2SS did not affect processing and N-methylation (Pugsley, 1993). Analyses of the PulG pilus structure and assembly show that E5 is not implicated in docking, but participates in fibre stabilisation. More precisely, once the protomer P has been extracted from the membrane, its E5 residue interacts with two lysine residues (K28 and K35) of protomer P^{-3} (Campos *et al.*, 2010; Nivaskumar *et al.*, 2014). However, the Ala substitutions of these Glu and Lys residues lead to strikingly different phenotypes: while *pulG*$^{K28A/K35A}$ mutants are fully functional in protein secretion, *pulG*^{E5A} mutants are completely defective. This and other data suggest an additional role for E5 in a step preceding the docking step in the pilus assembly pathway (Nivaskumar *et al*., 2014). With the exception of the interactions between EpsG and the AP

component EpsL in *Vibrio cholerae* T2SS that have been revealed by chemical cross-linking (Gray *et al.*, 2011), little is known about the early events of the assembly process. To shed some light on these steps, we sought to characterise interactions between minor and major pseudopilins and to identify AP components that directly interact with pseudopilins using the *K. oxytoca* T2SS as a model system. By combining bacterial two-hybrid and co-purification approaches with mass spectrometry and functional analyses, we identified several interacting partners of the *K. oxytoca* major pseudopilin PulG and revealed a novel role of the conserved pseudopilin residue E5, which holds important clues to the assembly mechanism of the T4P fibre family.

Results

Mass spectrometry analysis of PulG and PulG^{E5A} co-assembled into mixed pili

As mentioned above, earlier studies showed that residue E5 is not required for PulG processing or N-methylation (Pugsley, 1993), while studies of T4P suggest the opposite (Strom and Lory, 1991; Aas *et al*., 2007). The assembly-defective pilin variants with E5 residue substitutions have been shown to co-assemble into pili in the presence of wild type pilins (Pasloske, *et al.*, 1989; Aas *et al.*, 2007). However, while N-terminal sequencing of *Neisseria gonorrhoeae* T4P made of PilE wild type and E5L variants revealed under-methylation of the pilins, it was not clear whether this under-methylation was specific to PilE^{E5L} (Aas *et al*., 2007). To clarify the role of E5 in PulG, we used a similar approach and tested whether the assembly-defective PulG^{E5A} variant can be co-assembled into pili with PulG^{WT}. Therefore, we co-expressed the full set of genes encoding the Pul T2SS (on plasmid pCHAP8185, which includes PulG^{WT}) with the gene encoding assembly-defective PulG^{E5A} variant (on plasmid pCHAP7790, Table 1). The surface proteins were isolated from these bacteria and analysed by SDS-PAGE and Coomassie Blue staining (Experimental Procedures and Figure 1A). A prominent band of approximately 14.5 kDa, the molecular

mass of PulG, was present in the sheared fraction (Figure 1A, lane 1). This band was not present in samples from the negative control strain producing $PulG^{E5A}$ and the Pul T2SS lacking PulG (ΔG, Figure 1A, lane 2). The intensity of this band was higher in the strain where both plasmids carried the wild type copy of the *pulG* gene (Figure 1A, lane 3), compared to the strain carrying a Δ*pulG* version of T2SS complemented with wild type *pulG* (Figure 1A, lane 4). To test whether $PulG^{E5A}$ was co-assembled with $PulG^{WT}$, the gel slices corresponding to the 14.5-kDa band were excised from lanes 1 (strain producing $PulG^{WT}$ and $PulG^{E5A}$) and 4 (producing $PulG^{WT}$) and analysed for protein content using top-down mass spectrometry (analysis of intact proteins without any digestion) (Gault *et al.*, 2014; Gault *et al.*, 2015). For $PulG^{WT}$ sample (Figure 1B), two major peaks were found at 14607.56 and 14621.54 Da, corresponding to the molecular mass of PulG (theoretical Mr: 14607.51 Da) and methylated PulG (theoretical Mr: 14621.53 Da). For the $PulG^{WT}$ + $PulG^{E5A}$ sample (Figure 1C), two supplementary peaks corresponding to $PulG^{E5A}$ (experimental: 14549.49 Da; theoretical: 14549.50 Da) and methylated $PulG^{E5A}$ (experimental: 14563.53 Da; theoretical: 14563.52 Da) were observed.

To confirm the N-terminal methylation and presence of an alanine residue (A) instead of a Glu (E) at the 5^{th} position in the sequence, we performed High Energy Collision Dissociation (HCD) fragmentation of the (14^{+}) ions of both methylated PulG and methylated $PulG^{E5A}$. The MS/MS spectra are shown in Figure 2. The presence of series of b-type ions in both cases confirms without any ambiguity both the methylation of the N-terminus and the identity of the 5th amino acid.

These results show that $PulG^{E5A}$ can assemble into pili, provided it is co-produced with $PulG^{WT}$. This suggests that $PulG^{E5A}$ likely co-assembles with native PulG into mixed pili. The presence of methylated and non-methylated forms of both PulG variants in the pili shows further that methylation of pseudopilins is not required for assembly.

Differential requirements of residue E5 for the major and minor pseudopilin function

With the exception of the PulK subunit, which caps the priming complex, all minor pseudopilins in T2SS have the conserved E5 residue. Given its strong conservation among (pseudo)pilins, we wondered whether E5 was also essential for minor pseudopilin function. To address this question, we introduced E5A substitutions in minor subunits PulH, PulI and PulJ and assessed their ability to support PulA secretion in conditions of low, chromosome-like levels of *pul* gene expression. The results of three independent secretion assays are shown in Figures 3A and supplementary Figure S1, and their quantification is shown in Figure 3B. Under these conditions, the PulG^{E5A} variant was as defective for PulA secretion as the negative control strain lacking PulG (Figure 3A, lanes 1-6), as shown previously (Nivaskumar *et al*., 2014), The *pulH* deletion mutant supported a low level of PulA secretion (Figure 3A, lanes 11,12) confirming that PulH is required for efficient secretion in physiological expression conditions (Cisneros *et al.,* 2012a). Surprisingly, PulA secretion in the presence of the PulH^{E5A} variant was nearly abolished, suggesting a dominant negative effect of the *pulH^{E5A}* allele (Figure 3A, lanes 7-12). In contrast, E5A substitutions in minor pseudopilins PulI and PulJ did not affect their function (Figure 3A, lanes 13-18 and 19-24). Replacing the Met-5 with Glu in variant PulK^{M5E} had no effect on PulA secretion (Figure 3A, lanes 25-30), confirming previous results obtained in conditions of *pul* gene overexpression (Vignon *et al.*, 2003). Thus, the requirement for E5 appears to be specific to PulG and PulH pseudopilins, which are not part of the priming tip complex and have been implicated in the downstream steps of pseudopilus assembly (Cisneros *et al*., 2012a).

Pseudopilin interaction network

The PulJ-PulI-PulK complex presumably provides a template for PulH incorporation (Cisneros *et al*., 2012a), as suggested by the formation of the quaternary complex comprising all minor pseudopilin periplasmic domains in the *P. aeruginosa* Xcp T2SS (Yanez *et al*., 2008; Korotkov and Hol, 2008; Douzi *et al*., 2009). However, this complex did not interact with the globular domain of the major pseudopilin XcpT *in vitro* (Douzi *et al*., 2009),

leaving the question of the mechanism that couples the initiation and elongation stages of assembly open. Based on the findings of Hu and collaborators (Hu *et al.,* 2002), it has been proposed that the minor pseudopilin quaternary complex and the major pseudopilin interact instead though their hydrophobic segments (Douzi *et al*., 2009). To test this possibility and to characterise the pseudopilin interaction network, we employed the bacterial two-hybrid (BAC2H) approach that allows one to study interactions between full-length, membrane-embedded proteins (Karimova *et al.*, 1998). Using this method we had previously demonstrated interactions of PulI with PulJ and PulK (Cisneros *et al*., 2012a). In the present study, we fused the T18 and T25 fragments of adenylyl cyclase CyaA from *Bordetella pertussis* to the N-terminus of all five full-length mature pseudopilins and performed BAC2H assays (Experimental Procedures). Using T18-PulG as bait, we identified strong interactions with two minor pseudopilins, PulH and PulJ (Figure 4). When T18-PulH was used as bait, a specific interaction was observed only with T25-PulG. Although both T18-PulH and T25-PulH chimera consistently showed a tendency to interact with PulJ, these interactions were not statistically significant despite low P values (0.106 and 0.201, respectively) (Figure 4A and Supplementary Dataset 1). The T18-PulI chimera showed specific interactions with PulJ and PulK (Figure 4), in agreement with previous studies in several T2SSs (Cisneros *et al*., 2012a; Korotkov and Hol, 2008; Douzi *et al*., 2009). Conversely, T18-PulJ interacted with PulI (Figure 4A). In addition, T18-PulI, T18-PulJ and T18-PulK showed a weak interaction with PulG. Of note, only PulG formed homo-dimers in the BAC2H assay, consistent with the unique ability of major pseudopilins to form long homo-polymers (Durand *et al.*, 2005). The results of these analyses, summarised schematically in Figure 4B, reveal multiple novel contacts between PulG and minor pseudopilins. Overall, the data are compatible with the formation of complexes containing all five pseudopilin species.

Pseudopilin interactions with IM assembly platform components

Previous functional studies suggest that the minor pseudopilin complex primes fibre assembly and that it might activate the ATPase PulE that is associated with the assembly platform (AP) complex (Cisneros *et al*., 2012a). The AP is essential for T2SS function and contains multiple copies of IM proteins PulC, PulF, PulL and PulM (Py *et al*., 2001; Possot *et al*., 2000). To understand the physical and functional link between AP and the pseudopilin complex and to elucidate molecular details of the initiation and elongation steps of assembly, we assessed interactions between the pseudopilins and membrane-embedded AP components by using the BAC2H system. Therefore, we fused the T18- and T25- CyaA fragments to the N-terminal ends of full-length AP components PulC, PulF, PulL and PulM (Experimental Procedures). In the BAC2H assays, both T18-PulG and T25-PulG interacted specifically with the corresponding PulM- and PulF-CyaA chimera, but not with PulC-chimera. T18-PulG interacted very weakly with the T25-PulL, but the reciprocal pair did not interact (Figure 5A), which was surprising, given that their homologues in *V. cholerae*, EpsL and EpsG, interact in a cross-linking study (Gray *et al*., 2011). We confirmed that this was not due to non-functional PulL chimera, since the latter did interact with corresponding PulM hybrids (Figure 5A, black bars on the right), as expected based on previous studies (Possot *et al*., 2000; Buddelmeijer *et al.*, 2006). The results, summarized in Figure 5B, revealed strong and specific interactions of PulG with the PulM and PulF components of the assembly platform, suggesting their direct role in pseudopilus elongation.

Among the minor pseudopilins, PulH also interacted with PulF and PulM, although these interactions seem weaker than those observed between PulG and PulF or PulM, based on beta-galactosidase activity levels (Figure 5A). A weak "one-way" interaction was also detected between T18-PulK and T25-PulM chimera. In addition, PulF interacted weakly but significantly with PulI, PulJ and PulK in one out of two protein hybrid pairs. The high beta-galactosidase activity of strains producing T18-PulF and T25-PulF chimera in the BAC2H system (Figure 5A) shows a strong propensity of PulF for dimer formation.

The PulG^{E5A} and PulH^{E5A} variants are specifically defective in the interaction with PulM

Given the suggested role of E5A in an early step of the assembly process (Campos *et al*., 2010; Nivaskumar *et al*., 2014), we asked whether the E5A mutation affects interactions of PulG with one of the assembly factors. In BAC2H assay the PulG^{E5A} variant showed equal or stronger interaction signal with PulF, compared to native PulG, as indicated by the high beta-galactosidase activities of T18-PulG^{E5A} or T25-PulG^{E5A} hybrids (Figure 6A). In contrast, the same PulG^{E5A} hybrids showed a significantly decreased interaction with PulM (Figure 6A). These results suggest that mutation E5A specifically alters the interface between PulG and PulM. Likewise, while the E5A substitution in PulH did not affect the PulH-PulF interaction, it reduced the interaction with PulM, supporting a role of E5 in PulM binding (Figure 6B).

The PulG-PulM interaction data were further validated with native, full-length proteins. We analysed PulG interactions with PulM and the effect of the PulG E5A substitution using a co-purification approach. PulG-His$_6$, PulG^{E5A}-His$_6$ or PulG^{WT} were co-produced with PulM in the absence of other T2SS components (Experimental Procedures). Membrane proteins were extracted from these strains with Triton-X-100 and separated on the Ni-NTA columns. PulM was co-eluted with PulG-His$_6$ (Figure 7A, lanes 6-11). Despite the higher levels of the PulG^{E5A}-His$_6$ variant produced and retained on the column, the quantity of co-purified PulM was significantly reduced (Figure 7A, lanes 17-22). Quantification of the relative amounts of PulG and PulM shows that the amount of co-eluted PulM was reduced nearly ten-fold, relative to PulG-His$_6$ (Figure 7B). As shown in Figure 7A, PulG and PulM were present in very low amounts in the elution fractions when membrane proteins were extracted from the control strain producing untagged PulG (lanes 28-33), indicating very low nonspecific binding to the Ni-NTA resin.

The results of these affinity co-purification experiments were in good agreement with those of the BAC2H analysis, revealing specific binding of PulM to PulG *in vivo*. They confirm that the E5A substitution in PulG, which abolishes pseudopilus assembly and protein secretion, specifically affected the interaction between PulG and PulM.

Discussion

Archaeal pili and flagella, as well as bacterial T2SS, T4P and competence systems use similar machineries to assemble helical fibres from membrane-anchored (pseudo)pilin subunits, suggesting a common mechanism. The globular (pseudo)pilin domains, exposed on the fibre surface, show variability in size and sequence, presumably optimized to promote specific functions (Berry and Pelicic, 2014; Nivaskumar and Francetic, 2014; Shahapure *et al.*, 2014). In contrast, their hydrophobic segments are highly conserved, which might reflect constraints imposed by their biogenesis and assembly pathway (Campos *et al.*, 2013). For example, high hydrophobicity is key for efficient targeting to the SRP and Sec pathways during integral membrane protein biogenesis (Francetic *et al*., 2007; Arts *et al*., 2007) and additional constraints might be linked to specific interactions with the prepilin peptidase or with fibre assembly factors. Here we used the *Klebsiella* T2SS as a model to study pseudopilus assembly, focusing on the most conserved (pseudo)pilin residue E5 playing an essential role in this process.

Although the E5 residue is involved in pseudopilus stabilisation via long-range interactions, genetic data suggest it plays a critical role at a step preceding pseudopilin docking. Using two complementary mass spectrometry methods we demonstrated unambiguously that PulG^{E5A} co-assembles with PulG^{WT} into mixed PulG pili containing the methylated and non-methylated forms of PulG and PulG^{E5A}. This confirms previous findings that E5A substitution does not prevent N-methylation of PulG (Pugsley, 1993) and shows that methylation is not essential for pseudopilus assembly. This is in agreement with assembly of T4P in the methylase-deficient *pilD* mutants of *P. aeruginosa* (Pepe and Lory, 1998) and with the small amount of non-methylated PulG detected in T2SS pilus preparations (Köhler *et al.*, 2004). Compared to PulG^{WT}, the degree of N-methylated PulG^{E5A} was lower, which might be a consequence of *pulG* overexpression increasing the load on the methyl-transferase function of the prepilin peptidase PulO. Of note, the proportion of PulG^{E5A}

in the mixed pili was substantially lower than 50%, which could be explained by the dependence on PuG^{WT} for assembly, as well as by the predicted impact of the E5A substitution on fibre stability, due to the loss of long-range interactions with $K28^{P-3}$ and $K35^{P-3}$ (Nivaskumar *et al*., 2014). We propose that co-assembly of $PulG^{E5A}$ relies on its ability to form heterodimers with $PulG^{WT}$ *via* the previously characterised electrostatic contacts of conserved residues E44 and D48 of the incoming subunit (P^{-1}) with R87 and R88 of the P subunit incorporated in the PulG pilus (Campos *et al*., 2010; Nivaskumar *et al*., 2014). This association with $PulG^{WT}$ in the membrane would bypass the defect of $PulG^{E5A}$ possibly related to its targeting to the assembly site, as discussed below.

Pseudopilus assembly requires the formation of the PulJ-PulI-PulK priming complex, essential for protein secretion by the T2SS (Cisneros *et al*., 2012a). While our previous studies demonstrated the correlation between the formation of this complex and pseudopilus assembly activation (Cisneros *et al.,* 2012a; Cisneros *et al.,* 2012b), the molecular events linking the two processes have not been identified. To understand this link, we employed the BAC2H approach and characterised the network of interactions between full-length membrane-embedded pseudopilins and between individual pseudopilins and the AP components. The results confirmed the PulI-PulJ and PulI-PulK interactions observed *in vitro* in T2SSs from *Vibrio* (Yanez *et al.*, 2008), *E. coli* (Korotkov and Hol, 2008) and *P. aeruginosa* (Douzi *et al*., 2009). In the BAC2H assay, the full-length PulH showed only a weak tendency to interact with PulJ, although the periplasmic domains of their *Pseudomonas* homologues interacted *in vitro* (Douzi *et al*., 2009). In addition, contrary to the latter study, we identified direct contacts of PulG with PulH, which are in agreement with the results obtained in *Xanthomonas* T2SS studies (Hu *et al.*, 2002). In the *P. aeruginosa* T4P, the BAC2H analysis revealed very similar interactions between FimU, the PulH structural homologue, and the major pilin PilA, showing that these contacts are conserved in both systems (Nguyen *et al.*, 2015). Morover, in the same study, FimU also failed to interact with FimW, the PulJ equivalent in this T4P system. Finally, we also identified novel direct contacts of PulG with PulJ that are in good agreement with the proposed structural models wherein GspH, but also

GspG, could be docked directly to GspJ at the base of the tip complex (Korotkov and Hol, 2008). An interaction between PulG and PulJ might bypass the requirement for PulH, explaining the minor effect of *pulH* deletion on PulG pilus assembly (Cisneros *et al*., 2012a) and on PulA secretion (Sauvonnet *et al*., 2000) in conditions of *pul* gene overexpression. However, when the T2SS components are not overproduced, this requirement becomes more critical, consistent with the strongly defective PulA secretion in the absence of PulH (Figure 3). In addition, all minor pseudopilin subunits showed a weak tendency to interact with PulG in the BAC2H assay, which might explain the capacity of PulI-PulJ and PulI-PulK minor pseudopilin pairs to partially restore initiation of PulG assembly in *ΔpulHIJK* mutants (Cisneros *et al*., 2012a).

How do pseudopilins connect to the AP and with the associated ATPase, essential for fibre elongation? The results of our BAC2H analysis show that PulH and PulG, but not the other minor pseudopilins, interact specifically with two AP components, PulM and PulF, which might provide a basis for the recruitment of the initiation complex to the assembly site. We demonstrated that PulG and PulH interact with the conserved AP component PulF, presumably *via* TM segments of the two partners, given the absence of prominent periplasmic segments in PulF. In view of their high conservation, PulF and its equivalents in T4P assembly systems might be the main factors imposing restraints on the pilin primary sequence. The sequence conservation of pseudopilin TM segments is consistent with weak but significant binding of all minor pseudopilins to PulF in the BAC2H assay (Figure 5). Although we cannot exclude the possibility that these weak interactions anchor the PulJ-I-K priming complex to PulF, we favour the model wherein the quaternary minor pseudopilin complex binds to PulF via PulH. In addition, PulF showed a strong tendency to form dimers in this assay, consistent with the crystallography data (Abendroth *et al*., 2009) and with the observed oligomerisation of its homologue PilC from *Thermus thermophilus* (Karuppiah *et al.*, 2010). In the recent study of the *Myxococcus xanthus* T4P architecture by cryo-electron tomography, the PulF homologue PilC also appears to form a dimer (Chang *et al.*, 2016). During fibre elongation, PulF dimers could act as membrane scaffolds or docking sites for the

minor pseudopilin complex (or the nascent pilus) on one hand, and the incoming PulG subunits on the other, to facilitate assembly. In the large-scale BAC2H interaction study of T4P from *Neisseria meningitidis*, the major pilin PilE interacted with the PulF homologue PilG, and both PilE and PilG formed homodimers, much like PulG and PulF (Georgiadou *et al.*, 2012). In the *P. aeruginosa* and *Myxococcus xanthus* T4P, the PulF homologue called PilC interacts with the ATPase PilB (Takhar *et al.*, 2013; Bischof *et al.*, 2016), consistent with its role in transduction of mechanical energy generated by the ATPase. In the *E. coli* bundle-forming pili (Bfp) the ATPase activity of BfpD is stimulated by specific regions of the PulF homologue BpfE (Crowther *et al.,* 2005).

Importantly, the BAC2H results revealed interactions of PulG and PulH with the PulM component of the AP. Moreover, the direct interaction of native PulG and PulM was confirmed by a complementary co-purification approach. So far, PulM has been implicated in stabilization of PulL within the AP complex (Possot *et al*., 2000). While the results of the BAC2H analysis confirm PulM interaction with PulL, widely observed and well-studied in other T2SSs (Py *et al*., 2001; Johnson *et al*., 2007; Lallemand *et al.*, 2013), the strong and specific interactions with PulG and PulH reveal a novel role for PulM, possibly in pseudopilin recruitment to the assembly complex. Furthermore, we have shown that E5A substitutions in PulG and PulH interfere with their interactions with PulM in the absence of any other Pul factors, which implies that, in both cases, the E5 residue is a key feature of the PulG-PulM and PulH-PulM interfaces. These interaction defects caused by the E5A substitution likely account for the dramatic assembly defect of PulG^{E5A} variant. The trans-dominant effect of the *pulH*^{E5A} allele might be due to the reduced ability of PulH^{E5A} to target the priming complex to PulM, as discussed below. In contrast, residue E5 is dispensable for function of PulI and PulJ subunits, although it might provide optimal packing with the N-termini of the distal neighbouring pseudopilins in the complex, as proposed previously (Craig *et al.*, 2003).

Our results show that PulG interacts strongly and specifically with PulM, but only very weakly with PulL, which apparently contradicts the studies in *Vibrio,* showing that EpsG could be cross-linked with EpsL (Gray *et al*., 2011). This difference in interaction might reflect

differences between the *Vibrio* and *Klebsiella* T2SSs, or could be due to a difference in the techniques used to detect G-L interactions. The interaction of EpsG with EpsL was observed using chemical cross-linking, which might enhance and stabilize a weak or indirect association (Gray *et al*., 2011). Here, we identified direct associations of PulG with PulM and PulF in the absence of other T2SS components using BAC2H, and also, in the case of PulG and PulM, by co-purification in the presence of nondenaturing detergents. Nevertheless, both studies support a similar model wherein interactions of major pseudopilin with the L-M complex result in pilin recruitment to the assembly site.

The architecture of the T2SS, proposed based on partial high- and low-resolution structural data of individual components (McLaughlin *et al.*, 2012) is very similar to that of the *Thermus thermophilus* or *Myxococcus xanthus* T4P determined by cryo-electron tomography (Gold *et al.*, 2015; Chang *et al.*, 2016). In all models, the secretin and the AP components homologous to PulC, PulL and PulM delimit a cage-like compartment that encloses PulF within and connects directly with the ATPase PulE at its base. While cryoEM tomography shows that the pilus occupies the interior of this compartment, PilO (a PulM homologue) and its interacting partner PilN (corresponding to the transmembrane and periplasmic domains of PulL) were placed in the lower periplasmic ring surrounding the cavity (Chang *et al.,* 2016).

Integrated with the previous data, the results of this study allow us to propose a schematic working model of pseudopilus assembly initiation and elongation (Figure 8). In this model, one of the initial steps, following pseudopilin maturation by the prepilin peptidase, would be the assembly of the priming complex PulJ-PulI-PulK and its binding to PulH and PulG (step 1). Consistent with the direct binding of PulH and PulG to PulF, and with PulF self-interaction, this complex would associate with a dimer of PulF (step 2). In step 3, the pseudopilins and PulF would bind to PulM, outside or within the pre-assembled complex that includes the secretin PulD channel in the OM bound to the IM components PulC and PulL. An independent assembly of this latter complex is consistent with the results of cellular localisation studies of T2SS components fused to fluorescent protein tags (Buddelmeijer *et al.*, 2009; Lybarger *et al.,* 2009), as well as with the T4P cryo-electron tomography data

(Chang *et al.,* 2016). Importantly, association of PulM with PulF-pseudopilin complex requires residue E5 of PulG and PulH (Figure 8, step 3). Results of the T4P study by cryo-tomography suggest that the ATPase is recruited to the assembly site in the final step of the T4P complex biogenesis (Chang *et al.*, 2016). A similar order of assembly, in which the incorporation of the PulF-pseudopilin complex into the incomplete T2S machine would precede the recruitment of the ATPase PulE, is possible in T2SS (steps 4 and 5). However, there is an important difference between the two systems at the level of PulL, which corresponds to a fusion between PilM and PilN of T4P, leaving open a possibility that ATPase recruitment occurs independently of PulF.

During pseudopilus elongation, PulG, possibly in the form of dimers, would be recruited to the assembly site *via* interaction with PulM, through the critical residue E5 (step 6). PulG would dock to the available PulF "acceptor" site and bind to the membrane-embedded $PulG^{P+1}$ subunit incorporated in the pseudopilus. ATP hydrolysis could drive rotation of the pilus *via* PulF to spool the protomer P into the growing fibre (step 7), following the one-start helix assembly model that we proposed and described earlier (Campos *et al.*, 2010; Nivaskumar *et al.,* 2014). Fibre elongation would comprise cycles of targeting, docking and spooling events (steps 6 to 9).

Based on this model, we propose that co-assembly of $PulG^{E5A}$ relies on its ability to form heterodimers with $PulG^{WT}$, which would promote targeting to the assembly site (Campos *et al*., 2010; Nivaskumar *et al*., 2014). The trans-dominant effect of $PulH^{E5A}$ variant would be due to its association to pseudopilin-PulF complex but not to PulM. While providing testable hypotheses, this model raises numerous questions, notably those related to the mechanism of exoprotein substrate recruitment and transport. Whether a recruitment step accompanies uptake of exoprotein substrate molecules, or whether there are mechanisms that control substrate entry to the preformed assembly site, are only some of the questions that need to be addressed by further investigation.

The interaction network of pseudopilin subunits and assembly platform proteins in the inner membrane described here will provide the basis for further biochemical and structure

function analysis of pseudopilus biogenesis and its mechanistic link with T2SS-mediated protein secretion.

Experimental Procedures

Bacterial strains and plasmids

The *Escherichia coli* strain DH5α *[F' lacI^Q ΔlacZM15 pro+ Tn10)]* was used for recombinant DNA experiments. Strains PAP7460 *[Δ(lac-argF)U169 araD139 relA1 rpsL150 ΔmalE444 malG501]* and PAP5207 *[Δ(lac-argF)U169 araD139 relA1 rpsL150 pcnB::Tn10 (F' lacI^Q ΔlacZM15 pro+)]* were used for *pul* gene expression studies. The *Δcya* strain DHT1 (Dautin *et al.*, 2000) was used for bacterial two-hybrid experiments. The bacteria were grown in LB medium supplemented with antibiotics, as required: chloramphenicol (Cm) (25 μg ml^{-1}), ampicillin (Ap) (100 μg ml^{-1}) or kanamycin (Km) (15 or 25 μg ml^{-1}). The expression of the *pul* genes was induced by addition of 0.4 % maltose. Isopropyl-β-D-thiogalactoside was added to induce *lacZ* promoter-controlled gene expression in strain PAP5207.

Plasmid construction

Plasmids used in this study are listed in Table 1. Plasmid DNA purification, gel extraction and PCR product purification were performed using appropriate Qiagen kits. Restriction enzymes, DNA ligase and other molecular biology reagents were purchased from Fermentas or New England Biolabs. The high-fidelity Pwo polymerase (Roche) was used for PCR amplification and site directed mutagenesis using the modified Quick-change method. The list of oligonucleotides (synthesized by Sigma Genosys) used for cloning or site-directed mutagenesis is provided in Supplementary Table 1. To construct the BAC2H chimera, the *pul* genes were PCR-amplified using corresponding primers, treated with DpnI and cloned into

493 pKT25 and pUT18c vectors using *Kpn*I and *Eco*RI enzymes. All plasmids were sequenced
494 by GATC.
495
496 *Bacterial two-hybrid and statistical analysis*
497
498 Competent cells of strain DHT1 were co-transformed with pUT18C and pKT25 derivatives
499 and bacteria were grown for 48 h at 30°C on LB plates containing Ap and Km. Colonies were
500 picked at random and inoculated into 5 ml cultures in LB containing Km and Ap, grown
501 overnight and inoculated the next day into fresh medium containing 1 mM IPTG. Bacteria
502 were cultured to mid-log phase and β-galactosidase activity was measured as described
503 (Miller, 1972). At least 2 independent experiments were performed with 3 randomly picked
504 transformants. Mean values were presented by bar graphs, and error bars indicate standard
505 deviation. Microsoft Excel software was used for data processing and presentation. The
506 statistical analysis was performed using the non-parametric Kruskal-Wallis test, followed by
507 Dunn's post-test for multiple comparisons, using the Prism software.
508
509 *Purification of PulG pili*
510
511 PAP7460 bacteria were transformed with pCHAP8185 plasmid containing all *pul* T2SS
512 genes including *pulG*^{WT}, or its derivative pCHAP8184 lacking *pulG,* and with pSU18 or its
513 derivatives pCHAP1205 (PulG^{WT}) or pCHAP7790 (PulG^{E5A}) carrying different *pulG* alleles
514 under control of the *lacZ* promoter. Bacteria were cultured on LB agar containing Ap, Cm and
515 0.4 % maltose. After incubating for 48 h at 30°C, bacteria were harvested and resuspended
516 in LB medium. Pili were sheared by vortex treatment and 20 passages through a 26-Gauge
517 needle. Two consecutive centrifugation steps at 16 000 g for 20 min were used to separate
518 bacteria and pili. The pilus fractions were further collected by ultracentrifugation in rotor Ti60
519 at 150 000 g and pili were resuspended in 20 mM HEPES for further analysis by SDS-PAGE
520 and mass spectrometry.

Mass spectrometry

All samples were desalted by C_4 ZipTip® (Millipore) and eluted directly into a 10 µL spray solution of methanol:water:formic acid (75:25:3). Between 2 and 6 µL were introduced into an Orbitrap Velos mass spectrometer, equipped with ETD module (Thermo Fisher Scientific, Bremen, Germany) using a TriVersa NanoMate® (Advion) in positive ion mode. The spray voltage was set to 1.2-1.6 kV and back-pressure to 0.3-0.4 psi. A full set of automated positive ion calibrations was performed immediately prior to mass measurement. The transfer capillary temperature was lowered to 100°C, sheath and auxiliary gasses switched off and source transfer parameters optimised using the auto tune feature. Helium was used as the collision gas in the linear ion trap. The FT automatic gain control was set at $1x10^6$ for MS experiments. Spectra were acquired in the FTMS in full profile mode with between 10 microscans over several minutes, with averaging on and set to max, and a resolution of 60,000 at 400 m/z. The final few spectra were then averaged using Qualbrowser in Thermo Xcalibur 2.1 and deconvoluted using Xtract to produce zero charge mass spectra.

For MS/MS experiments, the FT automatic gain control was set at $2x10^5$. Ions corresponding to the isotopic distribution of a single charge state (14^+) were selected with the largest possible window to avoid overlap with neighbouring species but minimize signal loss. HCD was performed at 27 eV and spectra were acquired in the FTMS in full profile mode at a resolution of 60,000 at 400 m/z, with 10 microscans and with averaging on and set to the maximum value. The final few spectra were then averaged using Qualbrowser in Thermo Xcalibur 2.1 and deconvoluted using Xtract to produce singly charged MS/MS spectra. MS/MS spectra were interpreted manually.

SDS-PAGE and immuno-detection

548 Proteins from bacterial extracts were separated by electrophoresis on 9 % or 10 %
549 polyacrylamide gels and transferred onto nitrocellulose membranes (ECL, Amersham) using
550 a semi-dry blotting apparatus. Membranes were blocked with 5% milk in TBST (10 mM Tris,
551 150 mM NaCl, 0.05% Tween 20) and incubated with polyclonal antisera raised against
552 purified PulA, PulG and MalE-PulM (diluted 1:1000 in TBST-5% milk), followed by four 10-
553 min washes and incubation in horseradish peroxidase-coupled anti-rabbit antibody (1:40,000;
554 Amersham). Membranes were developed by enhanced chemiluminescence ECL2 (Thermo)
555 or Western Lightning Plus ECL (PerkinElmer) and recorded using the Typhoon phosphor-
556 imager (GE) or LAS 4000 imager (Fujifilm). ImageJ software (Abramoff *et al.*, 2004) was
557 used to quantify the density of bands.
558
559 *PulA secretion assay*
560
561 PAP5207 bacteria were transformed with pCHAP8185 plasmid derivatives containing *pul*
562 genes with corresponding pseudopilin gene knockouts, and a pSU18 empty vector or its
563 derivatives containing the missing wild type or mutant pseudopilin gene (Table 1). Bacteria
564 were grown in LB containing Ap and Cm in the presence of 0.4% maltose, 1/10 volume of M9
565 salts and 1 mM IPTG to early stationary phase (OD_{600nm} >2). Cultures were normalized to
566 OD_{600nm} = 1 and bacteria were pelleted by centrifugation for 10 min at 16000 g at 4°C.
567 Bacteria were resuspended in SDS-sample buffer at final concentration of 1 OD_{600nm} per ml.
568 Supernatant fractions were centrifuged again for 10 min and mixed with equal volume of 2x
569 SDS-sample buffer. Samples corresponding to 0.05 OD_{600nm} from each fraction were
570 separated by SDS-PAGE on 9% Tris-Tricine gels. Proteins were transferred to nitrocellulose
571 membranes (ECL Amersham) by semi-dry electro-transfer. Polyclonal antisera were used for
572 immuno-detection of PulA.
573
574 *Co-purification of PulG-bound proteins*
575

Bacteria of strain PAP7460 producing PulG-His_6, $PulG^{E5A}$-His_6 or $PulG^{WT}$ variants encoded by pCHAP1362, pCHAP7785 and pCHAP8658, respectively and PulM (from plasmid pCHAP2393) were cultured at 30°C in LB medium containing Cm and Ap to OD_{600nm} = 1. Bacteria were collected by centrifugation and broken by sonication in cold TBS (20 mM Tris-HCl, pH 7.4, 150 mM NaCl) with 100 µg.ml^{-1} of lysozyme. The lysate was cleared by centrifugation to remove unbroken debris. Membranes were collected by ultracentrifugation at 186000 x g and resuspended in cold TBS, followed by solubilisation with 2% Triton X-100. Ultracentrifugation was repeated at 150000 g to remove non-solubilised membranes. Ni-NTA resin beads were washed with ~10 volumes of TBS and the solubilised membrane fraction was incubated with Ni-NTA resin at 4°C. The flow-through was collected, followed by seven washes with two column volumes of TBS supplemented with 20 mM imidazole. Proteins were eluted with TBS containing 300 mM imidazole.

Acknowledgments

We thank Evelyne Richet for insightful comments and for the critical reading of the manuscript, Jenny-Lee Thomassin for the help with statistical analysis, Alexandra East and Peter J. Bond for helpful suggestions. We are grateful to all members of the Laboratory of Macromolecular Systems and Signaling and of the Laboratory of Intercellular Communication and Microbial Infections for helpful discussions and friendly support. We thank Gouzel Karimova and Daniel Ladant for strains, plasmids and advice concerning the BAC2H analysis. This work was funded by the ANR FiberSpace grant N°ANR-14-CE09-0004. MN was a scholar of the Pasteur-Paris University (PPU) International PhD Program. JSM is funded by a fellowship from the Basque Government. JCR and CM acknowledge the DIM MALINF from the Ile de France Region for funding the LTQ Orbitrap Velos. The authors declare that they have no conflict of interest.

References

Aas, F. E., H. C. Winther-Larsen, M. Wolfgang, S. Frye, C. Løvold, N. Roos, *et al*., (2007) Substitutions in the N-terminal alpha helical spine of *Neisseria gonorrhoeae* pilin affect Type IV pilus assembly, dynamics and associated functions. *Mol Microbiol.* **63**: 69-85.

Abendroth, J., M. Bagdasarian, M. Sandkvist and W. G. Hol, (2004a) The structure of the cytoplasmic domain of EpsL, an inner membrane component of the type II secretion system of *Vibrio cholerae*: an unusual member of the actin-like ATPase superfamily. *J Mol Biol* **344**: 619-633.

Abendroth, J., D. Mitchell, K. Korotkov, T. Johnson, A. Kreger, M. Sankvist, *et al*., (2009) The three-dimensional structure of the cytoplasmic domains of EpsF from the type 2 secretion system of *Vibrio cholerae*. *J Struct Biol* **166**: 303-315.

Abendroth, J., P. Murphy, M. Sandkvist, M. Bagdasarian and W. G. Hol, (2005) The X-ray structure of the type II secretion system complex formed by the N-terminal domain of EpsE and the cytoplasmic domain of EpsL of *Vibrio cholerae*. *J Mol Biol* **348**: 845-855.

Abendroth, J., A. E. Rice, K. McLuskey, M. Bagdasarian and W. G. Hol, (2004b) The crystal structure of the periplasmic domain of the type II secretion system protein EpsM from *Vibrio cholerae*: the simplest version of the ferredoxin fold. *J Mol Biol* **338**: 585-596.

Abramoff, M. D., P. J. Magelhaes andS. J. Ram, (2004) Image Processing with ImageJ. *Biophotonics Internatl* **11**: 36-42.

Aly, K., E. Beebe, C. Chan, M. Goren, C. Sepúlveda, S. Makino, *et al*., (2013) Cell-free production of integral membrane aspartic acid proteases reveals zinc-dependent methyltransferase activity of the *Pseudomonas aeruginosa* prepilin peptidase PilD. *Microbiologyopen* **2**: 94-104.

Arts, J., R. van Boxtel, A. Filloux, J. Tommassen and M. Koster, (2007) Export of the pseudopilin XcpT of the Pseudomonas aeruginosa type II secretion system via the signal recognition particle-Sec pathway. *J Bacteriol* **189**: 2069-2076.

Bartolomé, B., Y. Jubete, E. Martinez and F. de la Cruz, (1991) Construction and properties of a family of pACYC184-derived cloning vectors compatible with pBR322 and its derivatives. *Gene* **102**: 75-78.

Berry, J.-L. andV. Pelicic, (2014) Exceptionally widespread filaments composed of type IV pilins: the prokaryotic Swiss Army knives. *FEMS Microbiol Rev* **39**: 134-154.

Bischof, L. F., C. Friedrich, A. Harms, L. Søgaard-Andersen and C. van der Does, (2016) The type IV pilus assembly ATPase PilB of *Myxococcus xanthus* interacts with the inner membrane platform protein PilC and the nucleotide binding protein PilM. *J Biol Chem* **291**: 6946-57.

Buddelmeijer, N., O. Francetic and A. Pugsley, (2006) Green fluorescent chimeras indicate nonpolar localization of pullulanase secreton components PulL and PulM. *J Bacteriol.* **188**: 2928-2935.

Buddelmeijer, N., M. Krehenbrink, F. Pecorari and Pugsley, A.P. (2009) Type II secretion system secretin PulD localizes in clusters in the *Escherichia coli* outer membrane. *J. Bacteriol.* **191**: 161-168.

Camberg, J. L., T. L. Johnson, M. Patrick, J. Abendroth, W. G. Hol and M. Sandkvist, (2007) Synergistic stimulation of EpsE ATP hydrolysis by EpsL and acidic phospholipids. *The EMBO journal* **26**: 19-27.

Campos, M., D. Cisneros, M. Nivaskumar and O. Francetic, (2013) The type II secretion system - a dynamic fiber assembly nanomachine. *Res Microbiol* **164**: 545-555.

Campos, M., M. Nilges, D. A. Cisneros and O. Francetic, (2010) Detailed structural and assembly model of the type II secretion pilus from sparse data. *Proc Natl Acad Sci U S A.* **107**: 13081-13086.

Chang, Y.-W., Rettberg, L.A., Treuner-Lange, A., Iwasa, J., Sogaard-Andersen, L. and Jensen, G. (2016) Architecture of the type IVa pilus machine. *Science* **351**: aad2001.

Cisneros, D. A., P. J. Bond, A. P. Pugsley, M. Campos and O. Francetic, (2012a) Minor pseudopilin self-assembly primes type II secretion pseudopilus elongation. *The EMBO journal* **31**: 1041-1053.

Cisneros, D.A., Péhaut-Arnaudet, G. and O. Francetic, (2012b). Heterologous assembly of type IV pili by a type II secretion system reveals the role of minor pilins in assembly initiation. *Mol. Microbiol.* **84**: 805-818.

Costa, T. R. D., C. Felisberto-Rodrigues, A. Meir, M. S. Prevost, A. Redzej, M. Trokter, *et al*., (2015) Secretion systems in Gram-negative bacteria: structural and mechanistic insights. *Nat Microbiol Rev* **13**: 343-359.

Craig, L., R. Taylor, M. Pique, B. Adair, A. Arvai, M. Singh, *et al*., (2003) Type IV pilin structure and assembly: X-ray and EM analyses of *Vibrio cholerae* toxin-coregulated pilus and *Pseudomonas aeruginosa* PAK pilin. *Mol Cell* **11**: 1139-1150.

Craig, L., N. Volkmann, A. S. Arvai, M. E. Pique, M. Yeager, E. H. Egelman, *et al*., (2006) Type IV pilus structure by cryo-electron microscopy and crystallography: implications for pilus assembly and functions. *Mol Cell.* **23**: 651-662.

Crowther, L.J.A. Yamagata, L. Craig, J.A. Tainer and M.S. Donnenberg. (2005) The ATPase activity of BfpD is greatly enhanced by zinc and allosteric interactions with other Bfp proteins. *J. Biol. Chem.* **280**: 24839-24848.

Dautin, N., G. Karimova, A. Ullman and D. Ladant, (2000) Sensitive genetic screen for protease activity based on a cyclic AMP signaling cascade in *Escherichia coli. J Bacteriol* **182**: 7060-7066.

Douzi, B., E. Durand, C. Bernard, S. Alphonse, C. Cambillau, A. Filloux, *et al*., (2009) The XcpV/GspI pseudopilin has a central role in the assembly of a quaternary complex within the T2SS pseudopilus. *J Biol Chem* **284**: 34580-34589.

Durand, E., A. Bernadac, G. Ball, A. Lazdunski, J. Sturgis and A. Filloux, (2003) Type II protein secretion in *Pseudomonas aeruginos*a: the pseudopilus is a multifibrillar and adhesive structure. *J Bacteriol* **185**: 2759-2758.

Durand, E., G. Michel, R. Voulhoux, J. Kurner, A. Bernadac and A. Filloux, (2005) XcpX controls biogenesis of the *Pseudomonas aeruginosa* XcpT-containing pseudopilus. *J Biol Chem* **280**: 31378-31389.

Francetic, O., N. Buddelmeijer, S. Lewenza, C. A. Kumamoto and A. P. Pugsley, (2007) Signal recognition particle-dependent inner membrane targeting of the PulG pseudopilin component of a type II secretion system. *J Bacteriol* **189**: 1783-1793.

Gault, G., M. Ferber, S. Machata, A.-F. Imhaus, C. Malosse, A. A. Charles-Orszag, *et al*., (2015) *Neisseria meningitidis* type IV pili composed of sequence invariable pilins are masked by multisite glycosylation. *PLoS pathogens* **11**: e1005162.

Gault, J., C. Malosse, S. Machata, C. Millien, I. Podglajen, M. Ploy, *et al*., (2014) Complete posttranslational modification mapping of pathogenic *Neisseria meningitidis* pilins requires top-down mass spectrometry. *Proteomics* **14**: 1141-1151.

Georgiadou, M., M. Castagnini, G. Karimova, D. Ladant and V. Pelicic, (2012) Large-scale study of the interactions between proteins involved in type IV pilus biology in *Neisseria meningitidis*: characterization of a subcomplex involved in pilus assembly. *Mol Microbiol.* **84**: 857-873.

Gold, V.A.M.,R. Salzer, B. Averhoff and W. Külhbrandt. (2015) Structure of a type IV pilus machinery in the open and closed state. *eLife* **10**, 7554/eLife.07380.

Gray, M. D., M. Bagdasarian, W. G. Hol and M. Sandkvist, (2011) In vivo cross-linking of EpsG to EpsL suggests a role for EpsL as an ATPase-pseudopilin coupling protein in the type II secretion system of *Vibrio cholerae. Mol. Microbiol.* **79**: 786-798.

Hu, N.-T.,Leu, W.-M.,Lee, M.-S., Che, S.-C., Chen, A., Song; Y.-L. and Che, L.-Y., (2002) XpsG, the major pseudopilin in *Xanthomonas campestris*, pv. campestris forms a pilus-like structure between cytoplasmic and the outer membranes. *Biochem J.* **365:** 205-211.

Johnson, T. L., M. E. Scott and M. Sandkvist, (2007) Mapping critical interactive sites within the periplasmic domain of the *Vibrio cholerae* type II secretion protein EpsM. *J Bacteriol* **189**: 9082-9089.

712 Karimova, G., J. Pidoux, A. Ullmann and D. Ladant, (1998) A bacterial two-hybrid system
713 based on a reconstituted signal transduction pathway. *Proc. Natl. Acad. Sci. USA* **95**:
714 5752-5756.
715 Karuppiah, V., D. Hassan, M. Saleem and J. P. Derrick, (2010) Structure and oligomerization
716 of the PilC type IV pilus biogenesis protein from *Thermus thermophilus*. *Proteins* **78**:
717 2049-2057.
718 Kohler, R., K. Schafer, S. Muller, G. Vignon, K. Diederichs, A. Philippsen, *et al*., (2004)
719 Structure and assembly of the pseudopilin PulG. *Molecular microbiology* **54**: 647-664.
720 Korotkov, K., M. Sandkvist and W. Hol, (2012) The type II secretion system: biogenesis,
721 molecular archtecture and mechanism. *Nat Rev Microbiol* **10**: 336-351.
722 Korotkov, K. V. and W. G. Hol, (2008) Structure of the GspK-GspI-GspJ complex from the
723 enterotoxigenic *Escherichia coli* type 2 secretion system. *Nat Struct Mol Biol.* **15**: 462-
724 468.
725 Korotkov, K. V., T. L. Johnson, M. G. Jobling, J. Pruneda, E. Pardon, A. Heroux, *et al*.,
726 (2011) Structural and functional studies on the interaction of GspC and GspD in the
727 type II secretion system. *PLoS pathogens* **7**: e1002228.
728 Lallemand, M., F. Login, N. Guschinskaya, C. Pineau, G. Effantin, X. Robert, *et al*., (2013)
729 Dynamic Interplay between the periplasmic and transmembrane domains of GspL
730 and GspM in the type II secretion system. *PloS One* **8**: e79562.
731 Lybarger, S.R., T.L. Johnson,M.D. Gray, A.E. Sikora and M. Sandkvist. (2009) Docking and
732 assembly of the type II secretion complex of *Vibrio cholerae*. J Bacteriol. **191**:3149-
733 3161.
734 McLaughlin, L., R. Haft and K. Forest, (2012) Structural insights into the Type II secretion
735 nanomachine. *Cu Op Struct Biol* **22**: 208-216.
736 Miller, J. H., (1972) *Experiments in molecular genetics*. Cold Spring Harbor Laboratory, Cold
737 Spring Harbor, New York.
738 Nguyen, Y., S. Sugiman-Marangos, H. Harvey, S. D. Bell, C. L. Charlton, M. S. Junop, *et al*.,
739 (2015) *Pseudomonas aeruginosa* minor pilins prime type IVa pilus assembly and
740 promote surface display of the PilY1adhesin. *J Biol Chem* **290**: 601-611.
741 Nivaskumar, M., G. Bouvier, M. Campos, N. Nadeau, X. Yu, E. Egelman, *et al*., (2014)
742 Distinct docking and stabilization steps of the pseudopilus conformational transition
743 path suggest rotational assembly of type IV pilus-like fibers. *Structure* **22**: 685–696.
744 Nivaskumar, M. and O. Francetic, (2014) Type II secretion system: a magic beanstalk or a
745 protein escalator. *BBA* **1843**: 1568-1577.
746 Nunn, D. and S. Lory, (1991) Product of the *Pseudomonas aeruginosa* gene *pilD* is a prepilin
747 leader peptidase. *Proc Natl Acad Sci U S A* **88**: 3281-3285.
748 Parge, H.E., K.T. Forest, M.J. Hickey, D.A. Christensen, E.D. Getzoff and J.A. Tainer, (1995)
749 Structure of the fibre-forming protein pili at 2.6 A resolution. *Nature* **378**: 32-38.
750 Pasloske, B. L. and W. Paranchych, (1988) The expression of mutant pilins in *Pseudomonas*
751 *aeruginosa*: fifth position glutamate affects pilin methylation. *Mol Microbiol.* **2**: 489-
752 495.
753 Pasloske, B. L., D. G. Scraba and W. Paranchych, (1989) Assembly of mutant pilins in
754 *Pseudomonas aeruginosa*: formation of pili composed of heterologous subunits. *J*
755 *Bacteriol* **171:** 2142-2147.
756 Possot, O., G. Vignon, N. Bomchil, F. Ebel and A. P. Pugsley, (2000) Multiple interactions
757 between pullulanase secreton components involved in stabilization and cytoplasmic
758 membrane association of PulE. *J Bacteriol* **182**: 2142-2152.
759 Pugsley, A., (1993) Processing and methylation of PuIG, a pilin-like component of the
760 general secretory pathway of *Klebsiella oxytoca*. *Mol Microbiol.* **9**: 295-308.
761 Py, B., F. Loiseau and F. Barras, (2001) An inner membrane platform in the type II secretion
762 machinery of Gram-negative bacteria. *EMBO Rep.* **2**: 244–248.
763 Sandkvist, M., M. Bagdasarian, S. P. Howard and V. J. DiRita, (1995) Interaction between
764 the autokinase EpsE and EpsL in the cytoplasmic membrane is required for
765 extracellular secretion in *Vibrio cholerae*. *The EMBO journal* **14**: 1664-1673.

766 Sauvonnet, N., G. Vignon, A. P. Pugsley and P. Gounon, (2000) Pilus formation and protein
767 secretion by the same machinery in *Escherichia coli. EMBO. J.* **19**: 2221-2228.
768 Shahapure, R., R. Driessen, M. Haurat, S. Albers and R. Dame, (2014) The archaellum: a
769 rotating type IV pilus. *Molecular microbiology* **91**: 716-723.
770 Strom, M. and S. Lory, (1991) Amino acid substitutions in pilin of *Pseudomonas aeruginosa*.
771 *J Biol Chem* **266**: 1656-1664.
772 Strom, M., D. Nunn and S. Lory, (1993) A single bifunctional enzyme, PilD, catalyzes
773 cleavage and N-methylation of proteins belonging to the type IV pilin family. *Proc Natl*
774 *Acad Sci U S A.* **90**: 2404-2408.
775 Takhar, H., K. Kemp, M. Kim, P. L. Howell and L. L. Burrows, (2013) The platform protein is
776 essential for Type IV Pilus Biogenesis. *J Biol Chem* **288**: 9721-9728.
777 Vignon, G., R. Köhler, E. Larquet, S. Giroux, M. C. Prévost, P. Roux, *et al*., (2003) Type IV-
778 like pili formed by the type II secreton: specificity, composition, bundling, polar
779 localization, and surface presentation of peptides. *J Bacteriol.* **185**: 3416-3428.
780 Voulhoux, R., G. Ball, B. Ize, M. V. Vasil, A. Lazdunski, L.-F. Wu, *et al*., (2001) Involvement
781 of the twin arginine translocation system in protein secretion via the type II pathway.
782 *The EMBO journal* **20**: 6735-6741.
783 Yanez , M., K. Korotkov , J. Abendroth and W. G. J. Hol, (2008) The Crystal Structure of a
784 Binary Complex of two Pseudopilins: EpsI and EpsJ from the Type 2 Secretion
785 System of *Vibrio vulnificus*. *J. Mol. Biol.* **375**: 471–486.
786
787

788

789

790 **Table 1. Plasmids used in this study**

Name	Origin/resistance	Relevant markers	Source/reference
pUT18c	ColE1/Ap^R	p*lacZ*-T18	(Karimova *et al*., 1998)
pKT25	p15A/Km^R	p*lacZ*-T25	(Karimova *et al*., 1998)
pUT18c-Zip	ColE1/Ap^R	GCN4 (Leu zipper region) fused to T18	(Karimova *et al*., 1998)
pKT25-Zip	p15A/Km^R	GCN4 (Leu zipper region) fused to T25	(Karimova *et al*., 1998)
pSU18	p15A/Cm^R	*placZ, lacZ'*	(Bartolomé *et al.*, 1991)
pCHAP1205	p15A/Cm^R	pSU18 *pulG*	(Possot *et al*., 2000)
pCHAP1329	p15A/Cm^R	pSU18 *pulJ*	(Possot *et al*., 2000)
pCHAP1331	p15A/Cm^R	pSU18 *pulH*	(Possot *et al*., 2000)
pCHAP1351	p15A/Cm^R	pSU18 *pulI*	(Cisneros *et al*., 2012)
pCHAP1362	p15A/Cm^R	pSU18 *pulG-His*$_6$	(Kohler *et al*., 2004)
pCHAP2393	ColE1/Ap^R	pUC18 *pulM*	(Possot *et al*., 2000)
pCHAP6117	p15A/Cm^R	pSU18 *pulJ*^{E5A}	This study
pCHAP7330	ColE1/Ap^R	pUT18c *pulG*	(Nivaskumar *et al*., 2014)
pCHAP7332	p15A/Km^R	pKT25 *pulG*	(Nivaskumar *et al*., 2014)
pCHAP7785	p15A/Cm^R	pSU18 *pulG* ^{E5A}*-His*$_6$	This study
pCHAP7790	p15A/Cm^R	pSU18 *pulG*^{E5A}	This study
pCHAP8113	ColE1/Ap^R	pUT18c *pulC*	This study
pCHAP8119	p15A/Km^R	pKT25 *pulC*	This study
pCHAP8154	ColE1/Ap^R	pUT18c *pulM*	This study
pCHAP8155	p15A/Km^R	pKT25 *pulM*	This study
pCHAP8184	ColE1/Ap^R	pCHAP8185 *ΔpulG*	(Campos et al., 2010)
pCHAP8185	ColE1/Ap^R	*pulS, pulA*$_{NA}$ *pulB pulCDEFGHIJKLMNO*	(Cisneros *et al*., 2012)
pCHAP8201	ColE1/Ap^R	pCHAP8185 *pulH::kan*	(Cisneros *et al*., 2012)
pCHAP8209	ColE1/Ap^R	pCHAP8185 *pulJ::kan*	(Cisneros *et al*., 2012)
pCHAP8212	ColE1/Ap^R	pCHAP8185 *pulK::kan*	(Cisneros *et al*., 2012)
pCHAP8218	ColE1/Ap^R	pCHAP8185 *pulI::kan*	(Cisneros *et al*., 2012)
pCHAP8245	ColE1/Ap^R	pUT18c-*pulI*	(Cisneros *et al*., 2012)

pCHAP8246	ColE1/Ap^R	pUT18c *pulJ*	This study
pCHAP8247	ColE1/Ap^R	pUT18c *pulK*	This study
pCHAP8248	p15A/Km^R	pKT25 *pulI*	(Cisneros *et al*., 2012)
pCHAP8249	p15A/Km^R	pKT25 *pulJ*	(Cisneros *et al*., 2012)
pCHAP8250	p15A/Km^R	pKT25 *pulK*	(Cisneros *et al*., 2012)
pCHAP8256	ColE1/Ap^R	pUT18c *pulH*	This study
pCHAP8257	p15A/Km^R	pKT25 *pulH*	(Cisneros *et al*., 2012)
pCHAP8364	ColE1/Ap^R	pUT18c *pulF*	This study
pCHAP8365	p15A/Km^R	pKT25 *pulF*	This study
pCHAP8418	p15A/Cm^R	pSU18 *pulH*^{E5A}	This study
pCHAP8420	p15A/Km^R	pKT25 *pulG*^{E5A}	(Nivaskumar *et al*., 2014)
pCHAP8434	p15A/Km^R	pKT25 *pulH*^{E5A}	This study
pCHAP8446	ColE1/Ap^R	pUT18c *pulH*^{E5A}	This study
pCHAP8472	ColE1/Ap^R	pUT18c *pulL*	This study
pCHAP8484	p15A/Km^R	pKT25 *pulL*	This study
pCHAP8568	p15A/Cm^R	pSU18 *pulG*	This study
pCHAP8639	p15A/Cm^R	pSU18 *pulK*^{M5E}	This study
pCHAP8670	ColE1/Ap^R	pUT18c *pulG*^{E5A}	(Nivaskumar *et al*., 2014)

791

792

Figure Legends

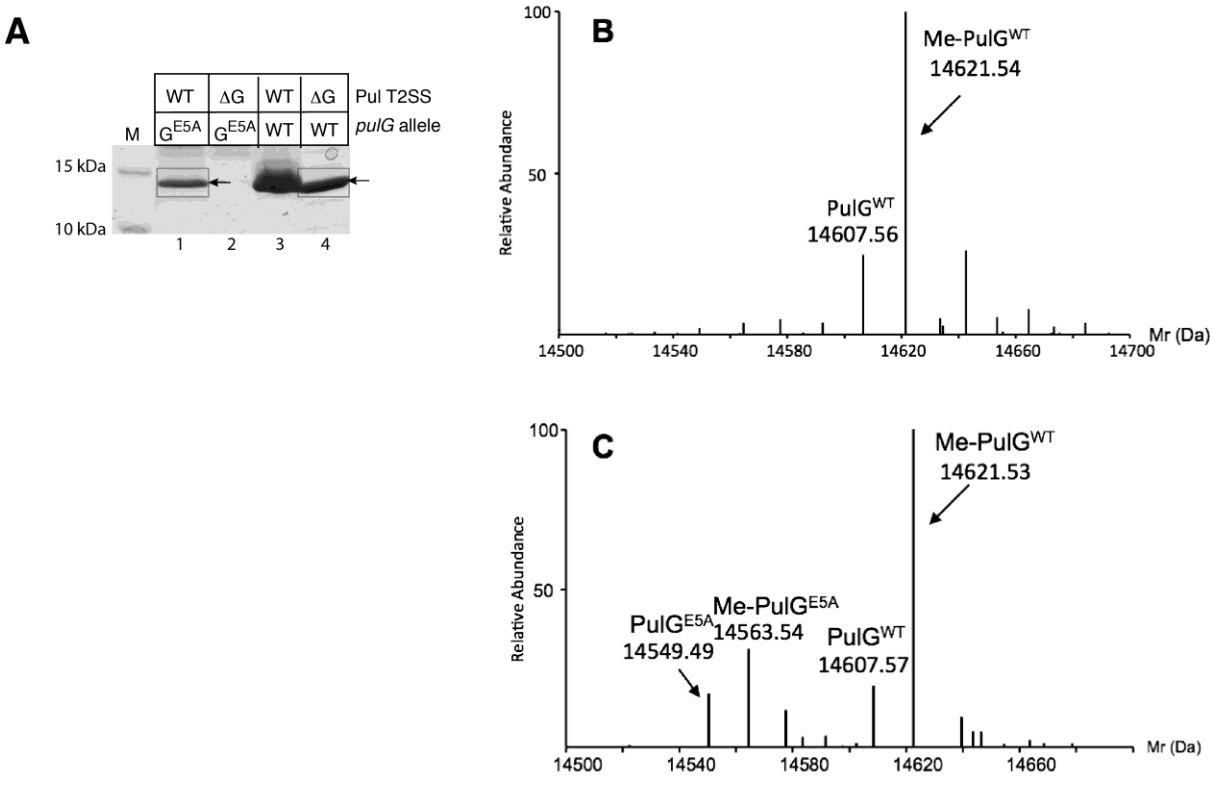

Figure 1. PulG^{E5A} is N-methylated and co-assembled into pili with PulG^{WT}. **A**. SDS-PAGE and Coomassie Blue stained sheared fractions from equivalent amounts of bacteria of strain PAP7460 carrying two compatible plasmids (Table 1), as indicated: lane 1, pCHAP8185 (encoding the complete Pul T2SS) and pCHAP7790 (encoding PulG^{E5A}); lane 2, pCHAP8184 (encoding Pul T2SS lacking PulG) and pCHAP7790; lane 3, pCHAP8185 and pCHAP1205 (encoding PulG^{WT}); and lane 4, pCHAP8184 and pCHAP1205. Only the relevant portions of the gel are shown, with the molecular mass markers indicated on the left. The expected molecular mass of PulG is around 14.6 kDa. The squares and arrowheads indicate samples that were further analysed by mass spectrometry. **B**. Deconvoluted high-resolution mass spectrum (in Mr) obtained for the sample in lane 4 (PAP7460 carrying *pulG*^{WT} allele) indicating the presence of a minor peak at 14607.56 Da corresponding to PulG^{WT} and a major peak at 14621.54 Da corresponding to methylated PulG^{WT}; **C**. Deconvoluted high resolution mass spectrum (in Mr) obtained for the sample in lane 1 (PulG^{WT} + PulG^{E5A}) indicating the presence of supplementary peaks corresponding to PulG^{E5A} (14549.49 Da) and methylated PulG^{E5A} (14563.53 Da).

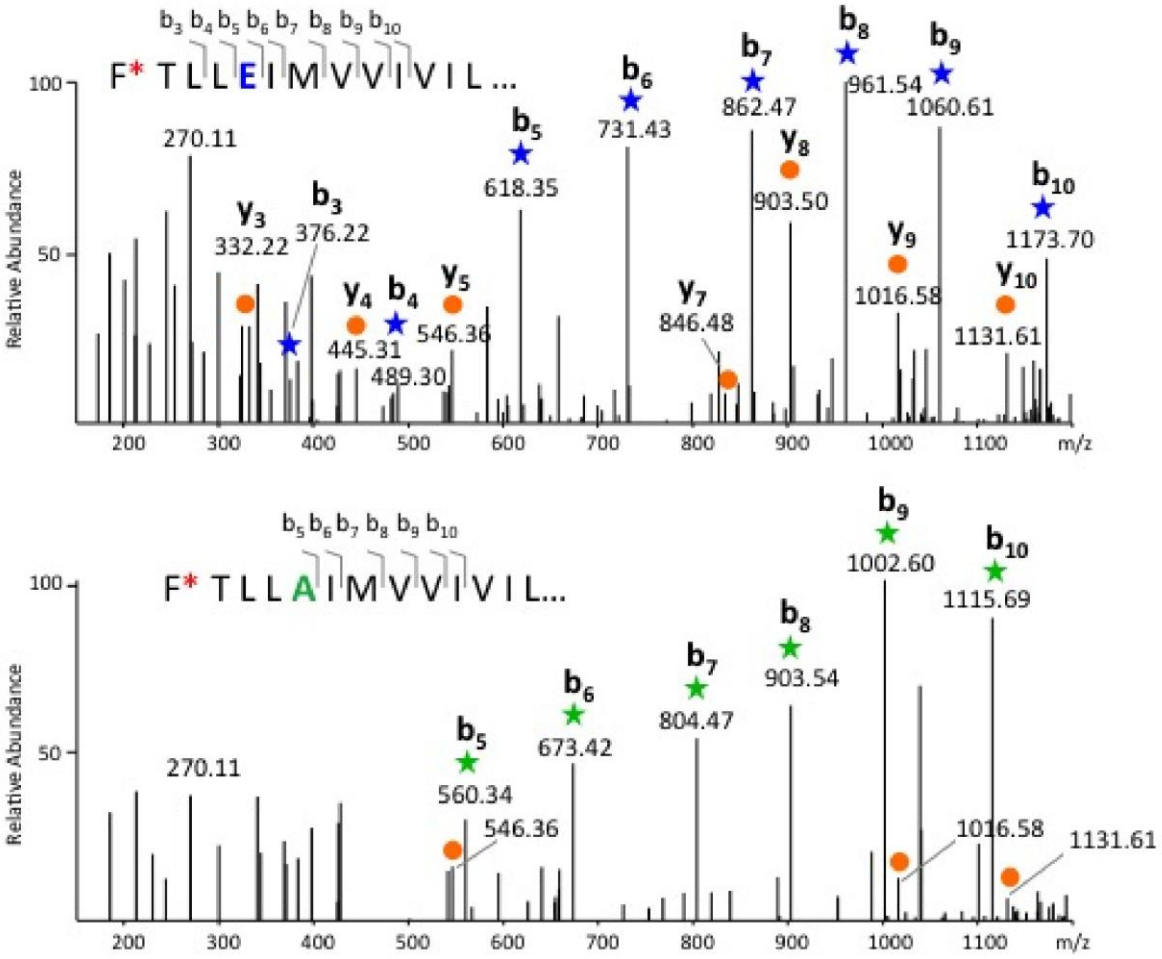

Figure 2. High-energy Collision Dissociation (HCD) analysis of methylated PulG^{WT} and PulG^{E5A} variants co-assembled into pili. HCD fragmentation spectra of the (14+) ion of methylated PulG^{WT} at 1046.05 (top) and methylated PulG^{E5A} at 1041.83 (bottom). Methylation of the N-terminal residue is indicated with an asterisk. The series of N-terminal b-type ions obtained in both cases and marked with a star unambiguously delineates the presence of an E at the 5th position in PulG^{WT} and an A in PulG^{E5A}. C-terminal y-type ions are depicted with a circle.

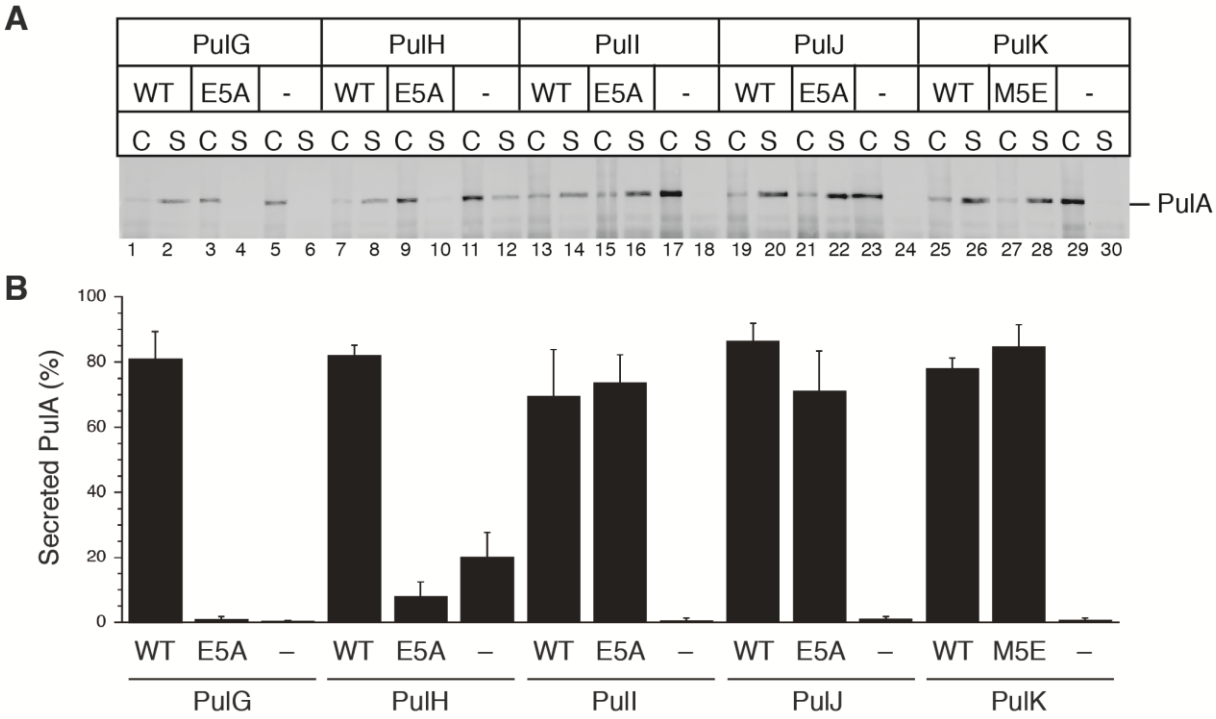

Figure 3. Effect of 5th residue substitutions on pseudopilin function. Pullulanase (PulA) secretion was assayed in *E. coli* strain PAP5207 containing pCHAP8185 derivatives with single deletions of pseudopilin genes was complemented with pSU18 plasmid (-) or its derivatives expressing the wild type (WT) or the mutant (E5A or M5E) allele of the missing pseudopilin gene as indicated above the lanes. **A**. A representative of three independent experiments is shown. Equivalents of 0.05 OD_{600nm} of cell (C) or supernatant (S) fractions were analysed on 9% Tris-Tricin SDS-PAGE and detected using anti-PulA antibodies. **B**. Quantification of the fraction of secreted PulA in the three independent experiments shown in panel A and in Figure S1. Bar graphs represent the mean values and the error bars indicate standard deviation.

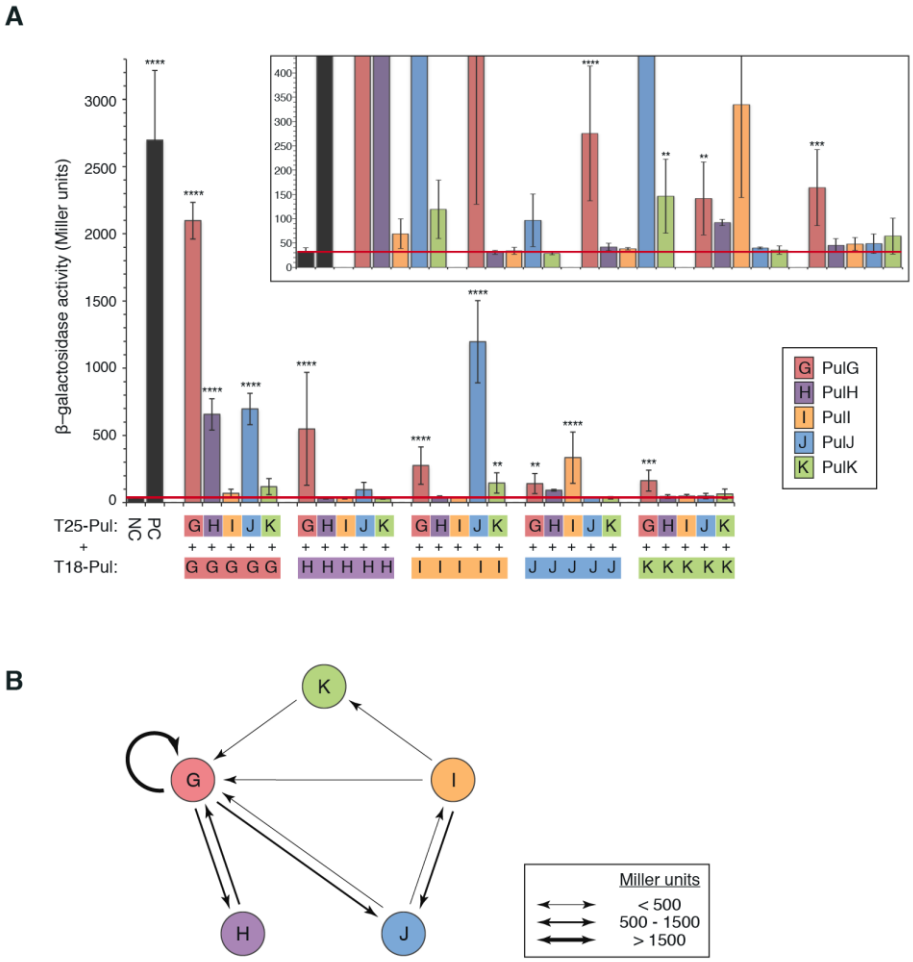

Figure 4. Pseudopilin interaction network determined by the bacterial two-hybrid analysis. **A.** Beta-galactosidase activities of DHT1 bacteria co-producing indicated T18 and T25 chimera determined as described in Experimental Procedures and expressed in Miller units. NC, activity of bacteria producing T18 and T25 as negative control; PC, activity of positive control strain producing T18-Zip and T25-Zip chimera. Each bar represents mean beta-galactosidase activity value from at least 3 independent colonies obtained by co-transformation of pKT25 and pUT18c derivatives encoding pseudopilin chimera (T25 or T18 fused to the N-terminus of mature pseudopilins) indicated by the colour code in the inset: PulG, red; PulH, purple; PulI, orange; PulJ, blue; and PulK, green. The colours of the bars correspond to the T25-fused proteins. The red horizontal line indicates the background mean beta-galactosidase activity measured in the negative control. Error bars indicate standard deviation. Statistical significance relative to the negative controls is indicated above graphs as follows: **** = p<0.001; *** = P< 0.01; * = P < 0.1; ns= non-significant. The inset above the main graph shows the part of the same graph with the scale of beta-galactosidase activities expanded in the low range (from 0 to 500 Miller units). **B.** The results are summarised schematically in a pentagram depicting pseudopilin arrangement in a putative right-handed helical complex. Arrows are oriented from T18- to T25- chimera and their line thickness indicates the strengths of significant interactions, in the range of beta-galactosidase activities (in Miller units) defined as shown in the legend: weak (50>mean>500), strong (500>mean>1500) and very strong (mean>1500).

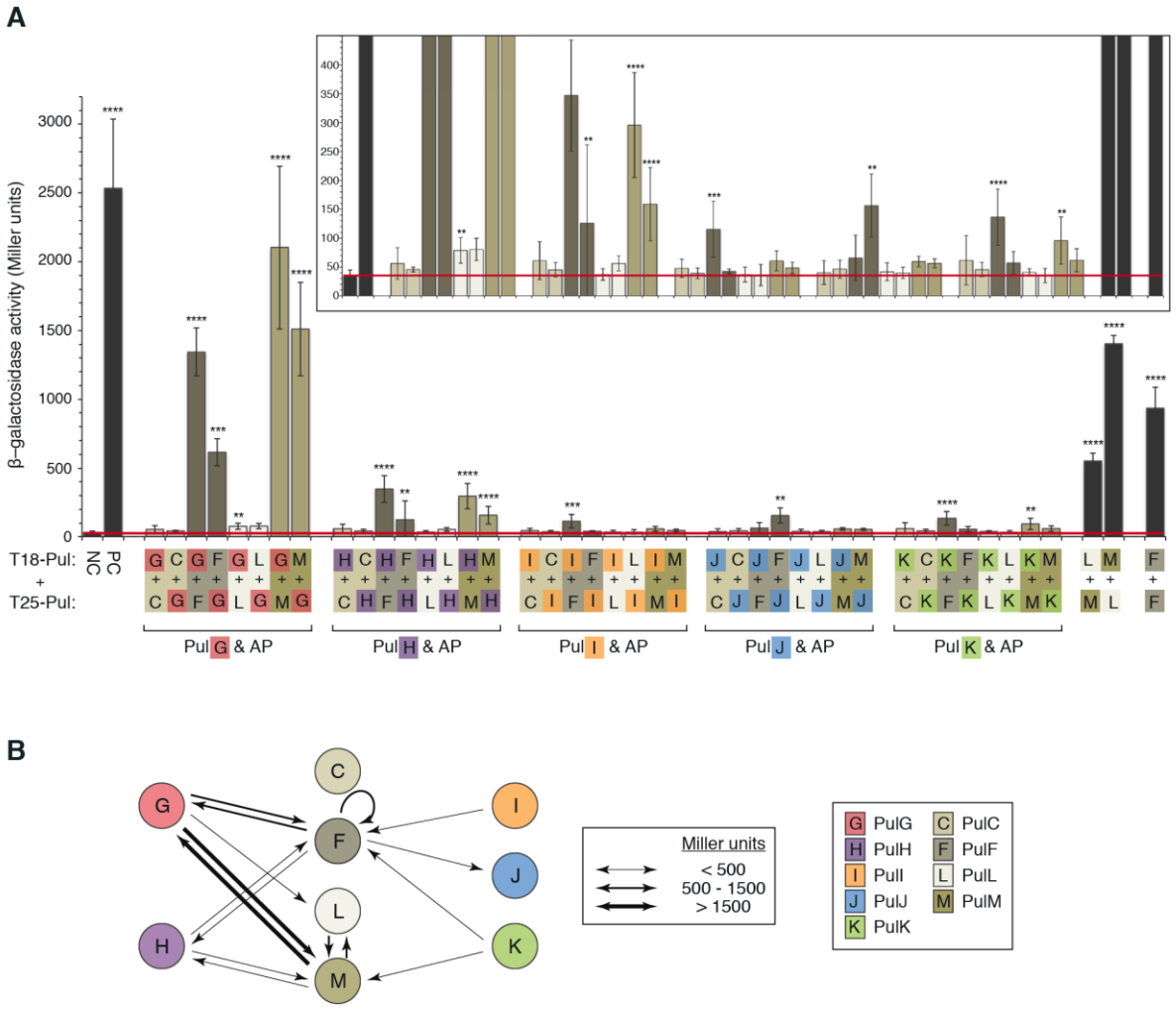

Figure 5. Interactions of pseudopilins with assembly platform components identified using bacterial two-hybrid analysis. **A**. Beta-galactosidase activities of DHT1 bacteria producing indicated T18-Pul or T25-Pul hybrids as bait in the presence of AP component chimera. The Pul components analysed are indicated by the single letter and colour code in the inset. NC, negative control strain co-producing T18 and T25 fragments; PC, positive control co-producing T18-Zip and T25-Zip chimera. The bars represent mean values from at least 3 independent colonies resulting from co-transformation of strain DHT1 with indicated pKT25 and pUT18c derivatives. The colours of the bars correspond to the AP proteins tested. The red line indicates the background beta-galactosidase activity measured in the NC. Error bars indicate standard deviation. Statistically significant mean values relative to the negative control (Experimental Procedures and Supplementary Dataset 1) are indicated above bars. The inset above the main graph shows the part of the same graph with the expanded scale of beta-galactosidase activities in the low range (from 0 to 500 Miller units). **B**. Summary of the interaction data, with the arrows oriented from T18- to T25- chimera and with line thickness corresponding to arbitrary range of interaction strengths indicated in the legend, as in Figure 4.

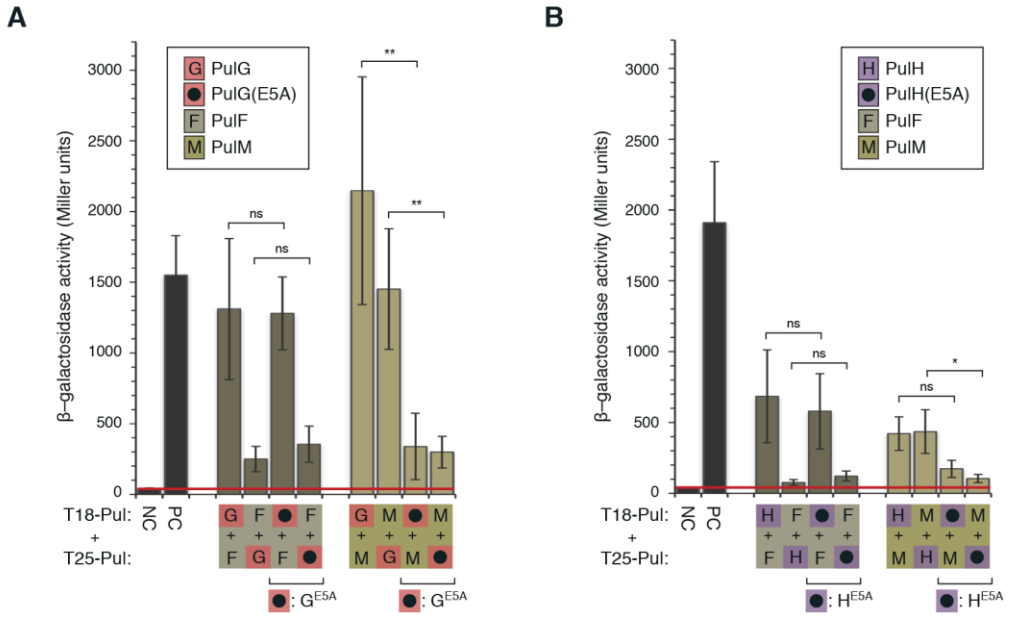

Figure 6. The effect of E5A substitution on PulG and PulH interactions with PulF and PulM. **A.** Bacterial two-hybrid analysis of PulG and PulG^{E5A} interactions with PulF and PulM. **B.** Bacterial two-hybrid analysis of PulH and PulH^{E5A} interactions with PulF and PulM. Each bar represents the mean value from at least 3 independent colonies obtained by transformation of pKT25 and pUT18c derivatives containing indicated inserts. The colours of the bars correspond to the AP proteins. Error bars indicate standard deviation. NC, negative control and PC, positive control as indicated in the legend of Figure 4. The red line indicates the background beta-galactosidase activity of the NC. Statistical significance of multiple pairwise comparisons is indicated by stars, as in Figure 4.

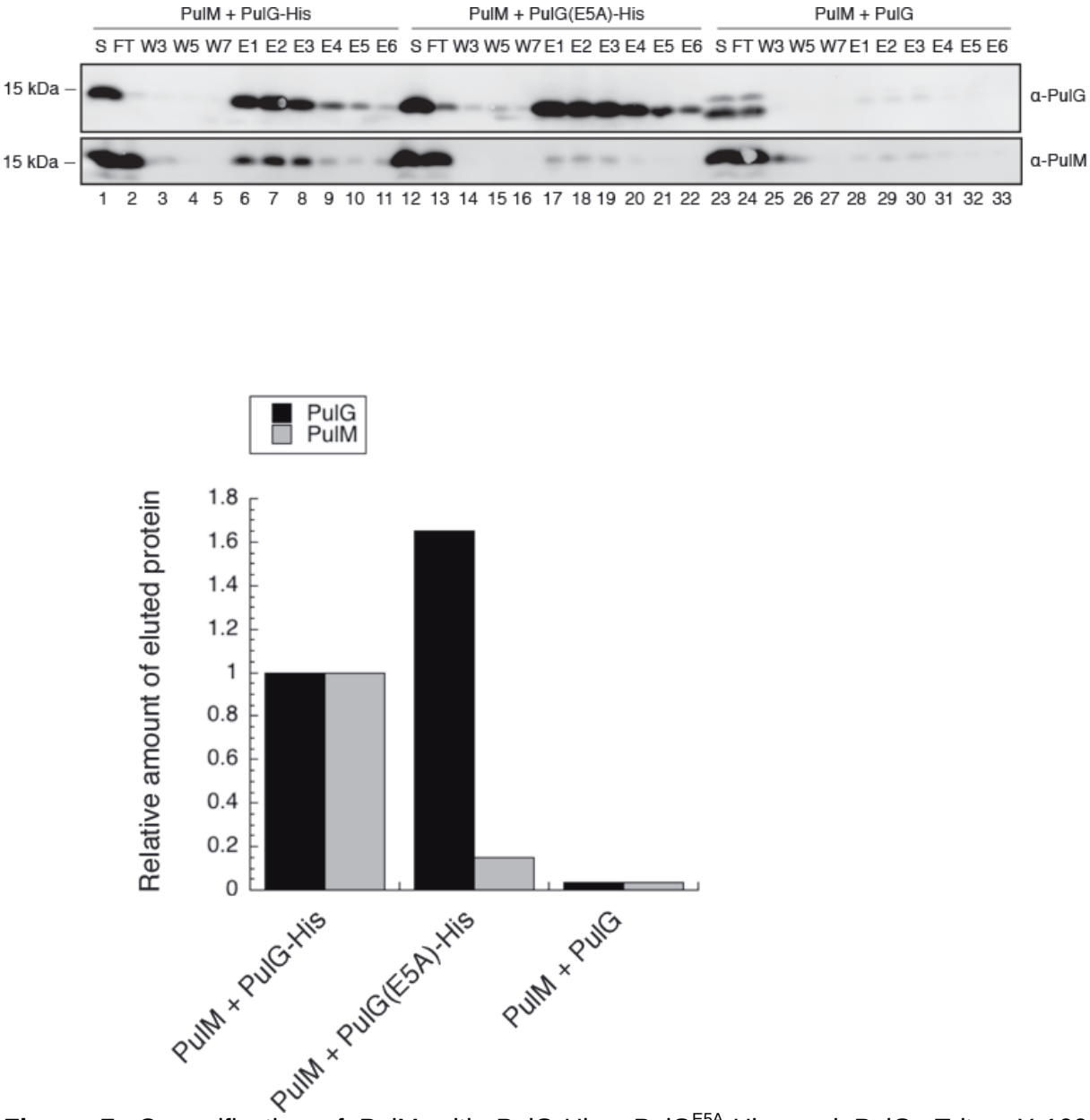

Figure 7. Co-purification of PulM with PulG-His_6, $PulG^{E5A}$-His_6 and PulG. Triton X-100 soluble extracts of total membranes from *E. coli* strains PAP7460 producing PulM and the indicated PulG variants were subject to affinity chromatography on Ni-NTA matrix (Experimental Procedures). **A**. SDS-PAGE and immuno-detection of PulG and PulM in fractions of the co-purification. S, solubilised membrane fractions; FT, flow-through; W1, W3 and W7, wash fractions; E1-E6, elution fractions. **B**. Quantification of the relative amount of eluted PulG and PulM relative to wild type levels, according to the densitometric analysis of the bands in (A).

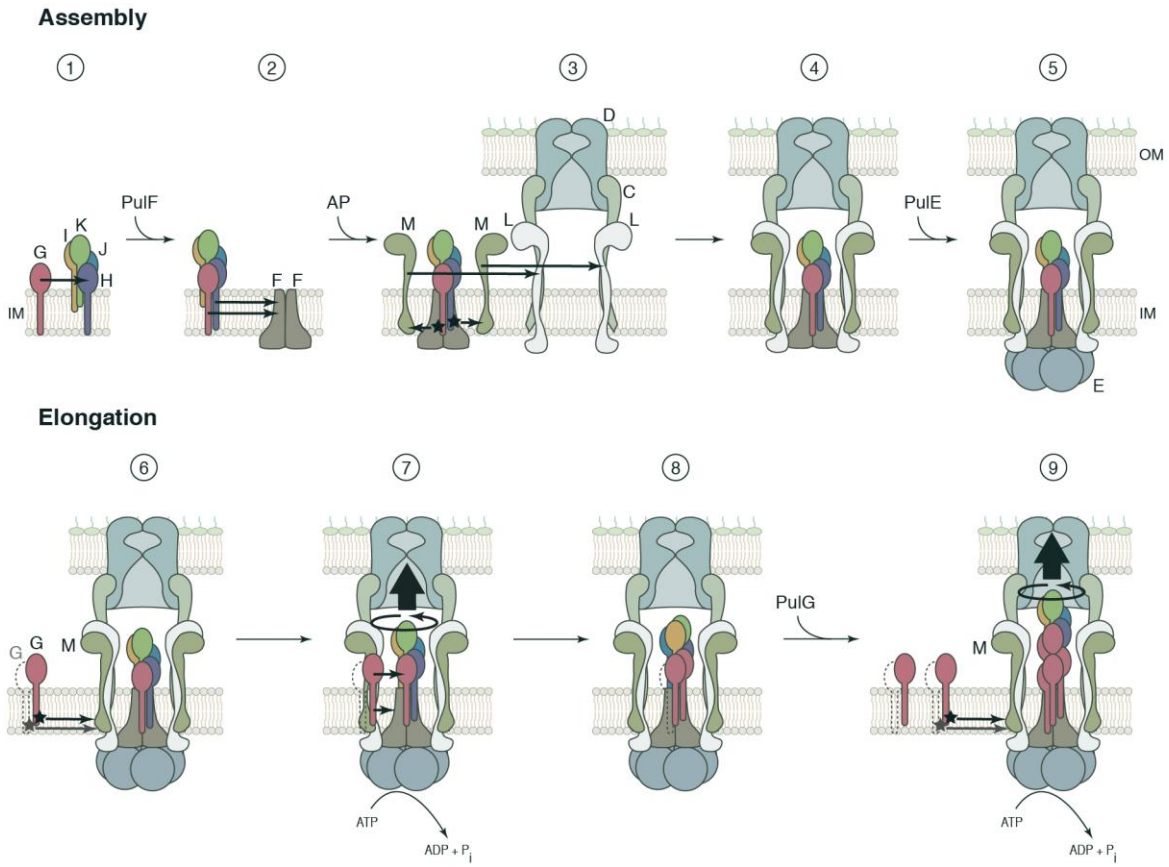

Figure 8. The working model of pseudopilus assembly and elongation. Assembly (top panel): Mature major pseudopilin PulG interacts with the quaternary complex composed of the priming PulJ-PulI-PulK trimer bound to PulH (step 1). Transmembrane regions of PulG and PulH drive the association of the pentameric *proto-pseudopilus* to a PulF dimer (2). PulM binds to this complex *via* the specific interactions of PulM with E5 residues of PulG and PulH, depicted as stars (3). The PulF-pseudopilin-PulM complex associates with PulL within the pre-assembled secretin PulD in the OM bound to the IM protein PulC. The initiation complex (4) recruits hexameric ATPase PulE via the cytoplasmic regions of PulL and possibly via PulF, thus resulting in a complete, functional T2S machine (5). Elongation (bottom panel): Fibre elongation begins with the recruitment of PulG subunits, likely in the form of dimers, by PulM (6). As in step 3, this recruitment requires a direct contact between the E5 residue of PulG and PulM (6). PulG enters the assembly platform, docks to PulF *via* its TM segments and associates with $PulG^{P+1}$ protomer of the proto-pseudopilus *via* their globular domains (7), through electrostatic contacts described previously (Nivaskumar *et al*., 2014). ATP hydrolysis causes conformational changes in PulE that are transmitted to PulF through direct contact, driving the rotation of the proto-fibre (7). The incoming PulG protomer is spooled into the fibre, which results in an overall extension of the pseudopilus (7 and 8). Fibre growth comprises multiple cycles of PulG recruitment, docking and extraction (steps 6 to 9).